

The Gas Study for the New Cylindrical Drift Chamber for the Systematic Investigation of Light Kaonic Nuclei

Y. KIMURA¹, T. AKAISHI², M. BAZZI³, P. BUEHLER⁴, A. CLOZZA³, C. CURCEANU³, H. FUJIOKA⁵, C. GUARALDO^{3†}, M. IIO⁶, M. ILIESCU³, K. INOUE², S. ISHIMOTO⁶, K. ITAHASHI⁷, M. IWASAKI⁷, T. HASHIMOTO⁷, S. KAWASAKI², G. KOJIMA¹, Y. MA⁷, Y. MAKIDA⁶, S. MANTI³, R. MURAYAMA⁷, T. NAGAE², T. NANAMURA⁸, H. NOUMI², H. OHHATA⁶, H. OHNISHI¹, M. OONAKA⁶, K. OZAWA⁶, F. SAKUMA⁷, K. SASAKI⁶, S. SASAKI¹, A. SCORDO³, F. SGARAMELLA³, K. SHIROTORI², D. SIRGHI³, F. SIRGHI³, N. SUMI⁶, K. SUZUKI², S. SUZUKI⁶, K. TANIDA¹⁰, K. TOHO¹, M. TSURUTA¹, T. YAMAGA⁶, M. YOSHIDA⁶, S. OKADA⁹, E. WIDMANN⁴, J. ZMESKAL^{4*}

¹*Research Center for Accelerator and Radioisotope Science (RARiS), Tohoku University, Sendai, 982-0826, Japan*

²*Research Center for Nuclear Physics (RCNP), Osaka University, Osaka, 567-0047, Japan*

³*Laboratori Nazionali di Frascati dell' INFN, I-00044 Frascati, Italy*

⁴*Stefan-Meyer-Institut für subatomare Physik, A-1090 Vienna, Austria*

⁵*Department of Physics, Institute of Science Tokyo, Tokyo, 152-8551, Japan*

⁶*High Energy Accelerator Research Organization (KEK), Ibaraki, 305-0801, Japan*

⁷*RIKEN, Saitama, 351-0198, Japan*

⁸*Department of Physics, Tohoku University, Sendai, 980-8578, Japan*

⁹*Chubu University, Aichi, 487-0027, Japan*

¹⁰*Japan Atomic Energy Agency (JAEA), Ibaraki 319-1195, Japan*

E-mail: y.kimura@raris.tohoku.ac.jp

(Received March 31, 2025)

The simplest kaonic nuclear-bound state, known as $\bar{K}NN$, was observed in the J-PARC E15 experiment. We are now entering a new phase in which we aim to investigate not only the existence of kaonic nuclei, but also their fundamental properties, such as spin-parity, decay branching ratios, and whether they genuinely exhibit high-density characteristics. To reveal these features, we plan to conduct a new experiment at J-PARC, the J-PARC E80 experiment, which is experiment to investigate the $\bar{K}NNN$ and expected to begin data-taking in 2027. For this experiment, a spectrometer has been designed to detect all decay particles from kaonic nuclei, including not only charged particles but also neutrons. The central detector for the E80 experiment is a large cylindrical drift chamber (CDC). The construction of the CDC has been completed, and it is now placed in the J-PARC assembly area. However, one issue regarding the detector gas filled in the CDC needs to be clarified. We have two candidates: one is Ar-C₂H₆ (at a 50:50 ratio), and the other is Ar-CO₂ (at a 90:10 ratio). A series of test measurements was conducted using both a radioactive source and cosmic rays. As a result, Ar-CO₂ (90:10) met our expected performance requirements in terms of detector efficiency and position resolution. Therefore, we began commissioning the new CDC filled with Ar-CO₂ (90:10) on October 2024.

KEYWORDS: kaonic nuclei, cylindrical drift chamber, gases for chamber, Ar-CO₂, Ar-C₂H₆

*Deceased.

1. Introduction

Protons and neutrons are fundamental constituents of matter, specifically atomic nuclei. In recent years, nuclei containing a Λ baryon have been studied experimentally. These nuclei are known as hypernuclei. Generally, such nuclei consist only of baryons. However, no nuclei containing a meson as a constituent—referred to as mesic nuclei—have been observed, despite theoretical predictions of their existence. The first clear evidence of mesic nuclei, namely an anti-kaon bound with two nucleons, was observed [1]. This state is known as the $K^- pp$ bound state ($I = 1/2$, $I_z = +1/2$). Nonetheless, the properties of kaonic nuclei remain largely unrevealed. For instance, the spin-parity has not yet been determined, and the existence of the isospin partner of $K^- pp$ has not been identified. Moreover, it is unclear whether additional kaonic nuclei with a higher number of nucleons exist, such as $\bar{K}NNN$ and $\bar{K}NNNN$. Theoretically, the existence of additional kaonic nuclei has been predicted; however, the evaluated binding energy and decay width vary significantly depending on the model. Therefore, new experimental data are essential to clarify their properties.

Moreover, the state of the kaonic nuclei is predicted to be compact due to the strong attraction of the $\bar{K}N$, which indicates that the high-density nuclear matter is realized in the system. The E15 results suggest that the $K^- pp$ could be quite compact system comparing to the mean nucleon distance of normal nuclei. By expanding this study to more heavier systems, we can conduct a systematic investigation of the system size via the form factor measurement, especially momentum transfer dependence on the mass number. Theoretical calculations on the system size utilizing different $\bar{K}N$ interaction models are still limited, so it is very important to obtain the information about the compactness experimentally.

We proposed a series of experiments to search for and investigate kaonic nuclei through (K^- , N/d) reactions on light nuclear targets at the J-PARC Hadron Experimental Facility K1.8BR beamline. As the first step, J-PARC E80 is planned in 2027. And the new detector system for the series of experiment from the J-PARC E80 is being built. In this paper, we report the status of one of the main detector in the new detector system, the cylindrical drift chamber (CDC), and the performance differences with different detector gases, namely Ar-C₂H₆ and Ar-CO₂.

2. J-PARC E80 experiment and Cylindrical Detector System

The $\bar{K}NN$ bound state was identified in the J-PARC E15 experiment in K^- induced reaction on ³He target by detecting all final state particles, i.e. Λpn in the reaction of $K^- + ^3\text{He} \rightarrow (\bar{K}NN) + n \rightarrow \Lambda p + n \rightarrow \pi^- + p + p + n$. The neutron in the final state has been identified by missing mass technique in the E15 experiment. The E80 experiment aims to search for the $\bar{K}NNN$ bound state via a reaction of $K^- + ^4\text{He} \rightarrow (\bar{K}NNN) + n \rightarrow \Lambda pn + n \rightarrow \pi^- + p + p + n + n$. Since two neutrons exist in the final state, the missing mass technique cannot be applied to identify and determine the kinematics of these two neutrons. Moreover, the number of final-state particles increases compared to the E15 case. Therefore, neutron detection efficiency and the detector acceptance need to be improved for the E80 experiment.

The conceptual design of the E80 spectrometer, referred to as the Cylindrical Detector System (CDS), is shown in Fig.1. All detectors are located inside a superconducting solenoid magnet. At the center of the CDS, the ⁴He target is placed. There is the Vertex Fiber Tracker (VFT) surrounding the target, which determines the Z-position of charged particles along the beam direction. Beyond the VFT lies the Cylindrical Drift Chamber (CDC), which tracks charged particles and analize their momenta. The outermost layer features the Cylindrical Neutron Counter (CNC). Further details on the E80 spectrometer can be found in Ref. [2].

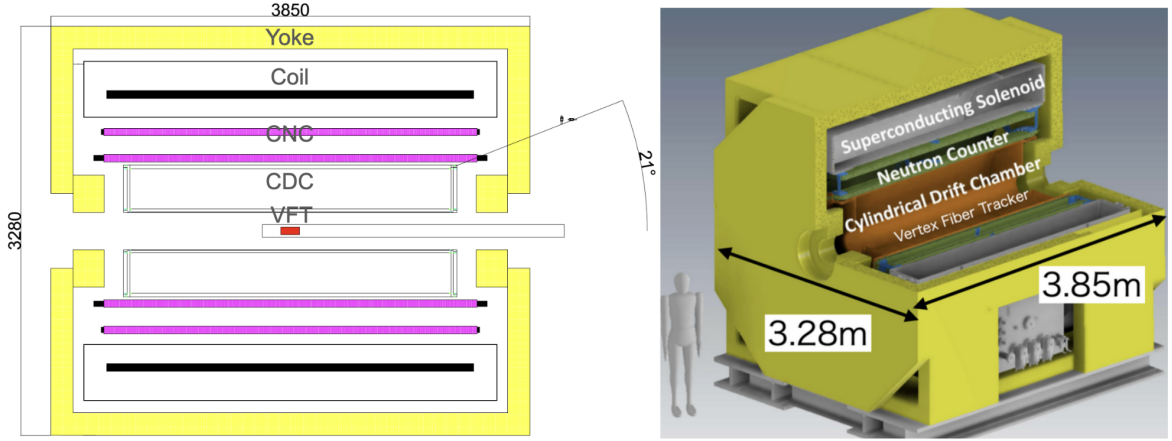


Fig. 1. Cross-sectional view of the design of the CDS. K^- beam comes from left side in this figure. Reaction point is determined by particle track of Beam Line Detectors, VFT and CDC. Momenta of the charged decay particles are also calculated using tracks in CDC with magnetic field. The role of the CNC are to identify of charged particle, to detect neutrons and to calculate momenta of the neutrons using TOF informations.

3. Cylindrical Drift Chamber

One of the main detectors in the CDS is the Cylindrical Drift Chamber (CDC). The role of the CDC is to detect decay particles from the produced kaonic nuclei, determine the reaction point from their trajectories, analyze the momentum of decay charged particles, and reconstruct the invariant mass of the kaonic nuclei using this information.

The structure of the CDC is shown in Fig. 2. The outer and inner radii are 530 mm and 150 mm, respectively, with a total mechanical length of 2,680 mm. The axial layer wires have a length of 2,580 mm, which provides an angular coverage of $21^\circ < \theta < 159^\circ$ in the polar angle region. This corresponds to a solid angle coverage of 93% of 4π . The CDC consists of two aluminum end plates, each 20 mm thick, supported by a 1 mm thick CFRP cylinder with an inner diameter of $\phi 303$ mm as the inner wall. There is no outer wall, but a 50 μm aluminized Mylar sheet is used to seal the gas volume. The Mylar sheet is supported by six CFRP pipes with an outer diameter of $\phi 18$ mm, which are attached to the outer periphery of the end plates.

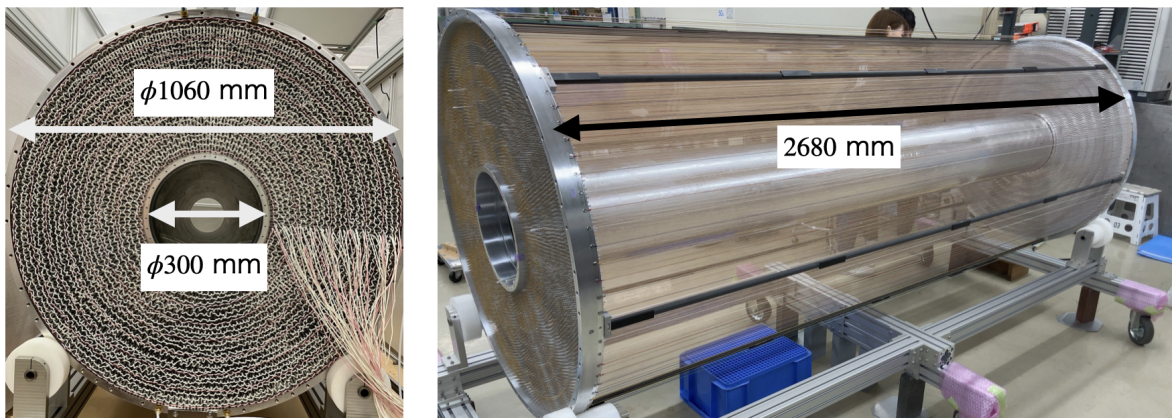


Fig. 2. Picture of the CDC before sealed by aluminized mylar. The CDC consists of two aluminum end plates and a CFRP cylinder as the inner wall. All the dimensions shown in Fig. 2 indicates not the active length but the mechanical length of the CDC.

The CDC has 15 layers of hexagonal cells with a typical drift length of 9 mm, grouped into seven superlayers, as shown in Fig. 3. And the cell structure of the new CDC is shown in Tab. I. In Fig. 3 and Tab. I, 'X' and 'U' layers are axial and stereo respectively. 'V' is also stereo layer which direction is opposite to 'U'. The eight stereo layers are tilted by approximately 2.7° to obtain longitudinal position information. The number of read-out channels is 1,816, and the total number of wires is 8,244. The CDC uses gold-plated tungsten(Au-W) wires with a diameter of $\phi 30 \mu\text{m}$ for the sense wires and beryllium-copper(Be-Cu) wires with a diameter of $\phi 80 \mu\text{m}$ for the field and guard wires. These wires are supported by feedthroughs with a bushing inserted at the ends and fixed by soldering. To keep the wire sag below $200 \mu\text{m}$, the Au-W and Be-Cu wires are tensioned at 70 g and 240 g, respectively. The total wire tension is 1.67 tons.

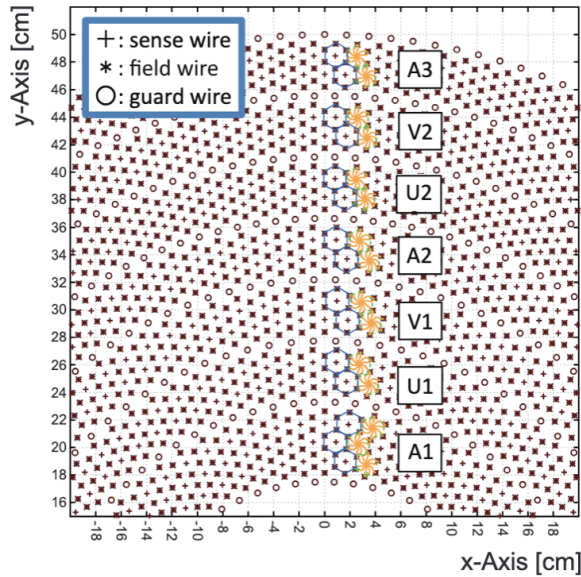


Fig. 3. Cell structure of the new CDC.

Table I. Cell configuration of the E80-CDC

Super-layer	Wire direction	Radius (mm)	Cell width (degree)	Cell width (mm)	Stereo angle (degree)	Signal channels per layer
A1	X	190.5	5.00	16.7	0	72
	X'	204.0		17.8	0	
	X	217.5		19.0	0	
U1	U	248.5	4.00	17.3	-2.27	90
	U'	262.0		18.3	-2.39	
V1	V	293.0	3.60	18.4	2.42	100
	V'	306.5		19.3	2.53	
A2	X	337.5	3.00	17.7	0	120
	X'	351.0		18.4	0	
U2	U	382.0	2.40	16.0	-2.82	150
	U'	395.5		16.6	-2.92	
V2	V	426.5	2.25	16.7	2.96	160
	V'	440.0		17.3	3.05	
A3	X	471.0	2.00	16.4	0	180
	X'	484.5		16.9	0	

4. What gas will be used?

In the E15 experiment, we used a mixture of Ar-C₂H₆ (50:50) gas for the CDC. However, this gas is flammable. Since the volume of the new CDC is three times larger than that of the CDC from the E15 experiment (E15-CDC), a non-flammable gas was considered for safety reasons.

4.1 Candidates for the filling gas

A mixture of Ar-CO₂ gas was selected as an alternative candidate for the detector gas. The gas simulation tool Garfield++¹ was used to investigate the drift velocity under various mixing ratios.

The drift velocity of Ar-CO₂ under some mixing ratio is shown in Fig. 4. For Ar-CO₂ mixtures, the drift velocity decreased as the Ar content increased. Among the tested ratios, the most stable drift velocity was observed for the Ar-CO₂ (90:10) mixture.

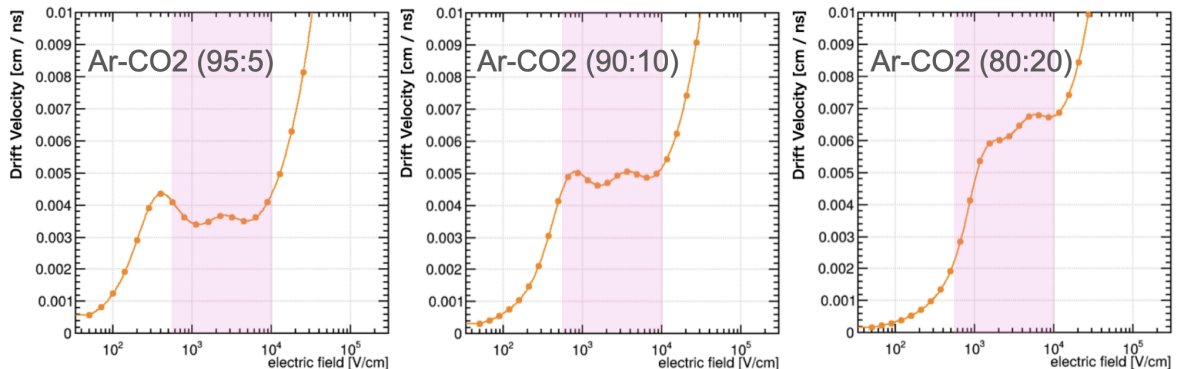


Fig. 4. Drift velocity of Ar-CO₂ under some mixing ratio. The drift region in case of the new CDC is in pink area. It is the most achieved that drift velocity is fast and stable in case of Ar-CO₂ (90:10).

Based on these results, we selected Ar-CO₂ (90:10) mixture was suitable for use in the drift chamber in terms of drift velocity. We conducted performance evaluation experiments using this gas mixture.

4.2 Measured gas gain

Gas gains of each gas mixture were measured using a ⁵⁵Fe source with a test chamber, which has the same cell structure of the new CDC to be reference for the following experiment. To evaluate the gas gain, a set of 1,000 direct waveforms from the sense wire was acquired using an oscilloscope. The signal charge Q was obtained by integrating the individual waveforms. When 5.9 keV X-rays from a ⁵⁵Fe source were irradiated onto the chamber, the number of primary electrons could be calculated. Given that the mean ionization energy W is 26 eV for Ar, 37 eV for CO₂, and 25 eV for C₂H₆, for example, the number of primary electrons n_T in an Ar-CO₂ (90:10) mixture is:

$$n_T = \frac{5.9 \times 10^3}{26} \times 0.90 + \frac{5.9 \times 10^3}{37} \times 0.10 = 2.2 \times 10^2$$

Letting Q denote the measured signal charge and e the elementary charge, the gas gain G is given by:

$$G = \frac{Q}{e \cdot n_T}$$

1. <https://garfieldpp.web.cern.ch/garfieldpp/>

The result of gas gain is shown in Fig.5. It was found that the Ar-CO₂(90:10) mixture can induce electron avalanches at lower applied voltages compared to the Ar-C₂H₆ (50:50) mixture. This trend is qualitatively consistent with simulation results obtained using Garfield++, where a gas gain of 1.0×10^4 was achieved at an applied voltage of 2150 V for Ar-CO₂ (90:10) and 2550 V for Ar-C₂H₆ (50:50). Although the absolute values differ, the relative ordering between the two gas mixtures agrees well, supporting the validity of the experimental observation.

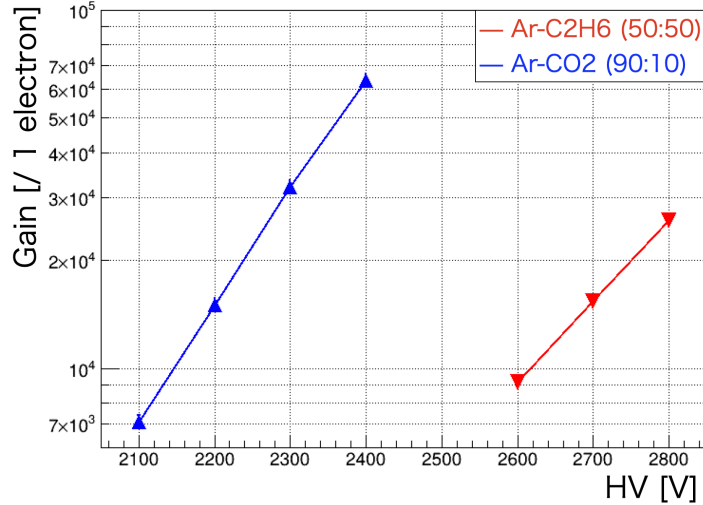


Fig. 5. Measured gas gain vs HV. The Ar-CO₂ (90:10) mixture is capable of initiating electron avalanches at lower voltages compared to the Ar-C₂H₆ (50:50) mixture. This result is in good agreement with the simulations performed using Garfield++

5. Cosmic-ray test with E15-CDC

To evaluate the overall performance of the CDC with Ar-CO₂ (90:10) gas, we conducted a comparative study using the CDC from the E15 experiment (E15-CDC) [3], which has the same structure as the new CDC except for wire length, filled with Ar-CO₂ (90:10) and Ar-C₂H₆ (50:50). The performance was assessed in terms of layer efficiency for charged particles and position resolution. In the E15 experiment, with a gas mixture of Ar-C₂H₆ (50:50), we achieved a layer efficiency of 97% and a position resolution of 200 μ m, which we adopted as the benchmark requirements for our detector.

5.1 Set up

Fig. 6 shows a schematic view of this test experiment. E15-CDC was used for this experiment. A two-fold coincidence in the top and bottom hodoscopes was employed for the trigger signal so that two tracks can be reconstructed in each event. For the Ar-C₂H₆ (50:50) gas mixture and Ar-CO₂ (90:10) gas mixture, the applied high voltage to each layer was set in the range of from -2500 to -2800 V and from -2150 to -2400 V respectively.

The readout system was identical to the one that will be used in the E80 experiment. The CDC's readout system operates as follows. The signal from the sense wire is first sent to the Amplifier-Shaper-Discriminator (ASD, SONY CXA3183Q, $\tau = 16$ ns) card, where it is processed and converted into a logic signal [4].

The Hadron Universal Logic Module (HUL) is used for the TDC module. The module's lowest bit resolution is set to 0.833 ns. The HUL supports a multi-hit TDC function, allowing up to sixteen hits to be recorded per event. Additionally, both the leading and trailing edges of the logic signal can be recorded. This enables charge information to be reconstructed in offline analysis based on the time interval between the leading and trailing edges.

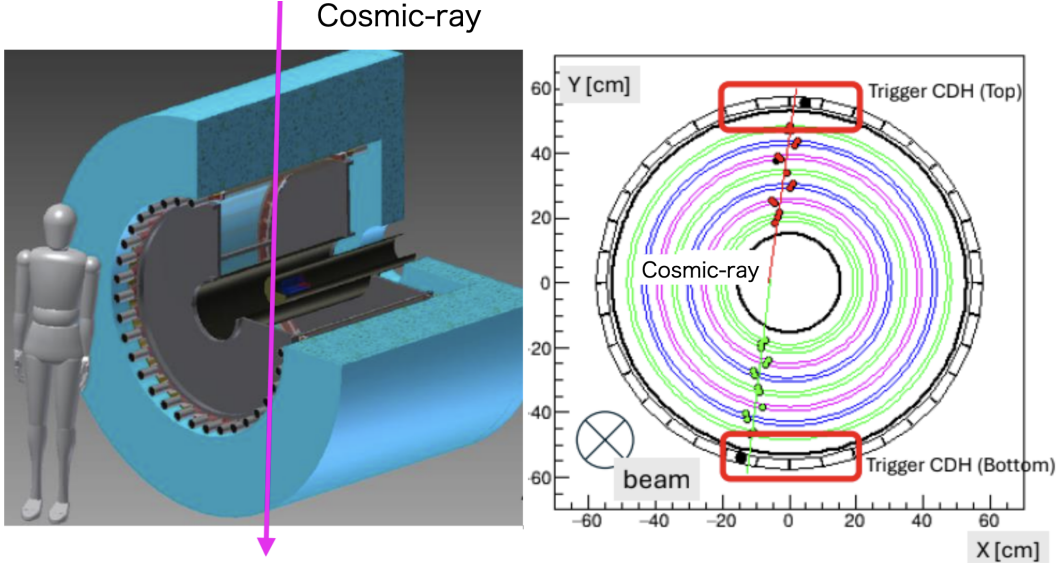


Fig. 6. (left): A schematic view of the E15-CDS. (right): An example of the event display of a cosmic-ray. Two tracks were reconstructed in each event under this condition, namely two multiplicity was required in each layer.

5.2 Analysis

The correlation between Time-Over-Threshold (TOT) and drift time, without applying any selection cuts, is shown in Fig. 7. The number of used events is 100,000 in both cases. These reveal that noise hits with low TOT values (TOT < 30, for example), which are not correlated with drift time, are clusterized in this region. For tracking purposes, hits with TOT < 30 were excluded (in case of Ar-C₂H₆ (50:50) applied -2400 V). A comparison between the two gas mixtures clearly indicates that the signal-to-noise (S/N) ratio of Ar-C₂H₆(50:50) at -2800 V is substantially lower than that of Ar-CO₂(90:10) at -2400 V.

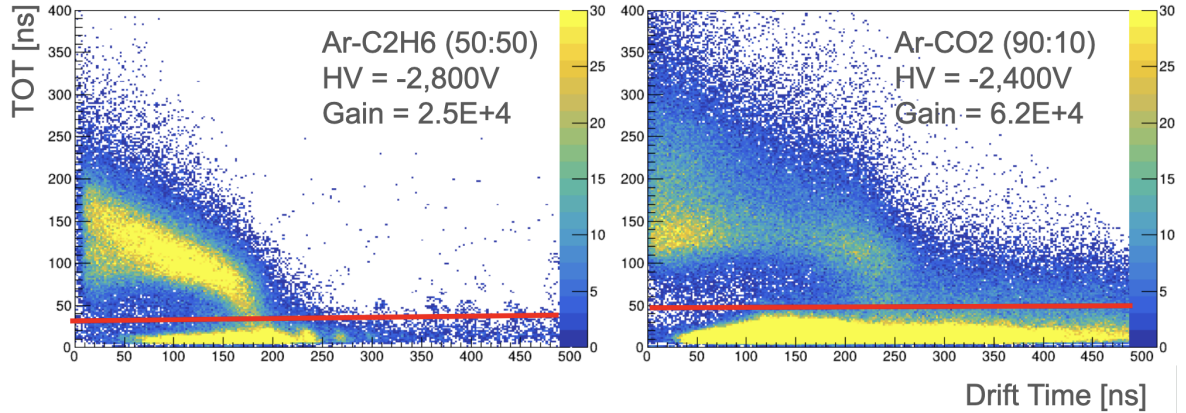


Fig. 7. Two-dimensional plots of TOT versus drift time. The left plot corresponds to Ar-C₂H₆(50:50) at -2800 V, while the right plot corresponds to Ar-CO₂(90:10) at -2400 V. Red line is the TOT threshold to reject the noise when tracking.

Drift time distribution and XT curve is shown in Fig.8 and Fig.9 respectively. The XT curve, representing the relationship between drift time and position, provides a means to convert timing information into spatial coordinates, with its slope corresponding to the local drift velocity. The difference between Ar-CO₂ (90:10) and Ar-C₂H₆ (50:50) can be seen clearly in Fig.8. On the other hand, both of the drift velocity, namely the slope of the XT curve is almost the same (~ 0.005 cm/s). In particular, it can be seen that the drift velocity of Ar-CO₂ (90:10) is consistent with the simulation results (in Fig.4). The same is true for Ar-C₂H₆ (50:50), which is omitted in this paper.

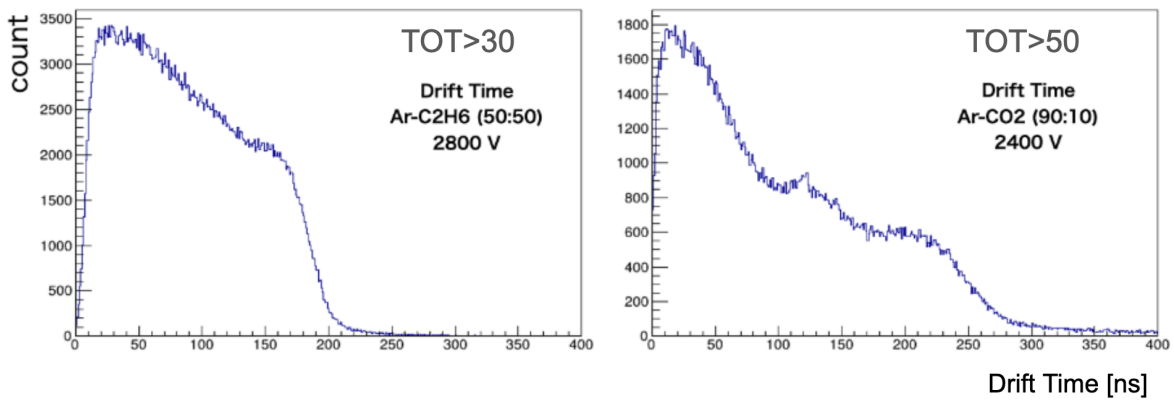


Fig. 8. Distribution of drift time after TOT cut.

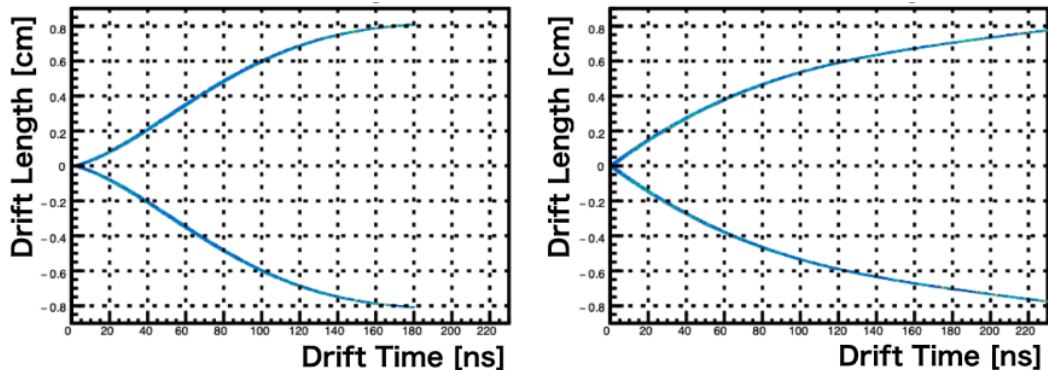


Fig. 9. The XT curve. This is used to convert timing information into spatial information.

Furthermore, to preferentially select ideal events, only events with a multiplicity of two were considered for each layer, and only the first hit on each wire was used for tracking. How to reconstruct a track is as follows:

- (1) Clusters are formed within each super-layer. A cluster is defined as a group of hits on adjacent wires across different layers in the same super-layer. Even a single isolated hit is treated as a cluster of size one.
- (2) Tracking begins using only clusters in the axial layers.
- (3) A track is reconstructed only if each axial super-layer (specifically super-layers 0, 3, and 6) contains at least one and fewer than 100 clusters. Furthermore, the product of the cluster counts from these three super-layers must be less than 10,000.
- (4) For each event, all possible combinations of clusters from the axial super-layers are considered. Within each cluster combination, the track candidate with the best χ^2/ndf is selected.

- (5) Once an axial track is found, nearby clusters in the stereo layers are searched. If qualifying clusters are found, tracking is repeated using all hits from both axial and stereo clusters. The same cluster selection criteria as in the axial case are applied to the stereo layers. If the total number of clusters across all layers (axial + stereo) is fewer than 10, no track is reconstructed. The final track is chosen as the one with the best χ^2/ndf among all combinations.

Then, the detection efficiency for each layer (layer efficiency) is defined by;

$$\text{Efficiency of Layer} \#X = \frac{N_{\text{track}}^{\text{all}}}{N_{\text{track}}^{\text{all}} + N_{\text{track}}^{\text{w/o } X}}$$

Here, $N_{\text{track}}^{\text{all}}$ represents the number of events in which tracks were reconstructed using all 15 layers, whereas $N_{\text{track}}^{\text{w/o } X}$ corresponds to the number of events in which tracks were reconstructed using all layers except for the target layer $\#X$.

And then, residual which is proportional to the spatial resolution of wire drift chamber is defined by;

$$\text{Residual} = D_{\text{track}} - l_D$$

Here, D_{track} represents the distance between the track and the sense wire, whereas l_D corresponds to the drift length.

5.3 Result

Using the reconstructed tracking information, we evaluated the layer efficiency and the residuals under various high voltage settings. For the Ar-C₂H₆ (50:50) gas mixture, high efficiency was achieved even at relatively low amplification voltages, as shown in Fig. 10. In contrast, the Ar-CO₂ (90:10) mixture exhibited a sharp increase in efficiency within the voltage range of -2300 V to -2350 V. To ensure that all 15 layers meet the required efficiency criteria, the high voltage must be set to -2400 V.

From Fig.11, as the high voltage increases, the sigma of the residual distribution decreases. The residual sigma saturates at approximately -2400 V for Ar-CO₂ (90:10) and -2800 V for Ar-C₂H₆ (50:50). Both gas mixtures yield comparable values in the range of 150–170 μm . If these values are interpreted as spatial resolution, the estimated layer resolution is less than 200 μm . The Ar-CO₂ (90:10) mixture exhibited detection efficiency and spatial resolution comparable to those of Ar-C₂H₆ (50:50), fulfilling the performance criteria required for our application.

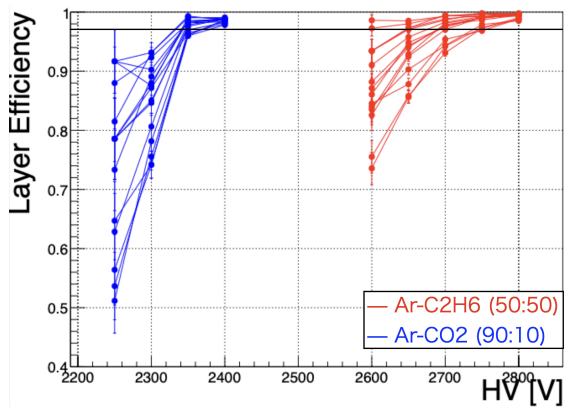


Fig. 10. Layer efficiency vs HV for each layer. The black line represents our required efficiency 97%. These gases met our required value, but higher gain was needed in case of Ar-CO₂ (90:10).

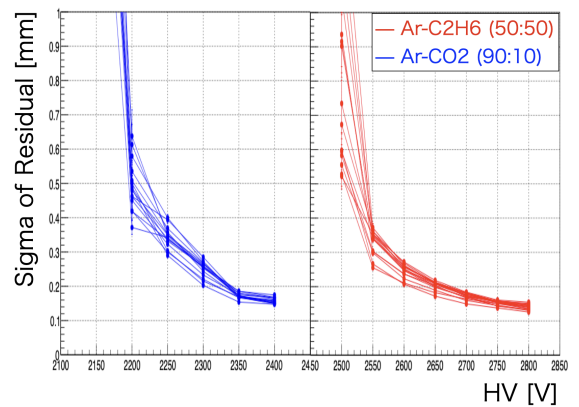


Fig. 11. Sigma of residual vs HV. The trend was similar between Ar-CO₂ (90:10) and Ar-C₂H₆ (50:50), but the residual of Ar-C₂H₆ (50:50) was a little bit better than that of Ar-CO₂ (90:10).

6. Summary and Prospects

In summary, we are planning a series of experiments at the J-PARC K1.8BR beamline to search for light kaonic nuclei such as $\bar{K}NNN$ and $\bar{K}NNNN$ as well as to measure the spin-parity of the $\bar{K}NN$ bound state. As the first step of this program, we are preparing for the J-PARC E80 experiment, which aims to search for the bound state of $\bar{K}NNN$. In the J-PARC E80 experiment, a newly developed large cylindrical drift chamber (Cylindrical Drift Chamber, new CDC) with a beam-axis length of approximately 2.8 meters has been constructed. The new CDC is a key detector for momentum measurement, which is essential for the full kinematic reconstruction of the decay charged particles from such kaonic nuclei.

The new CDC has a volume approximately three times larger than the CDC used in the previous E15 experiment (E15-CDC). Due to safety concerns associated with the flammability of the previously used Ar-C₂H₆ (50:50) gas mixture, an alternative nonflammable gas mixture of Ar-CO₂ is being considered for use in the new CDC. In this paper, we evaluate the fundamental gas properties of the Ar-CO₂ mixture as a candidate for the new CDC filling gas. We also compare its performance with that of the previously used Ar-C₂H₆ (50:50) mixture.

In order to evaluate the performance of Ar-CO₂ (90:10) as a filling gas in the CDC, cosmic-ray measurements were conducted using the E15-CDC, which is already in operation and shares the same cell structure as the new CDC. The E15-CDC was filled with an Ar-CO₂ (90:10) gas mixture. As a result, the Ar-CO₂ (90:10) mixture was confirmed to satisfy the required performance benchmarks: a detection efficiency of approximately 97% and a spatial resolution of around 200 μm . Based on these results, we conclude that the Ar-CO₂ (90:10) mixture is suitable for use in the new CDC. However the S/N ratio of Ar-C₂H₆ (50:50) was better than that of Ar-CO₂ (90:10). Therefore, we need a further discussion about the final decision whether or not we will use Ar-CO₂.

Recently, a cosmic-ray test was carried out using the new CDC filled with Ar-CO₂ (90:10), and cosmic-ray tracks were successfully reconstructed with the ASD electronics partially installed in December 2024. Next, we will fully install the ASD readout cards and proceed with full commissioning. These efforts are part of the ongoing preparations for the J-PARC E80 experiment, which aims to search for the $\bar{K}NNN$ bound state and is scheduled to commence in 2027.

Acknowledgment

This project is partially supported by MEXT Grants-in-Aid 17H04842, 19J20135, 21H00129, 18H05402, 26287057, 22H04917 and 24H00029.

References

- [1] T. Yamaga *et al.*, *Phys. Rev.*, C102, (2020) 044002
- [2] Technical Design Report on the J-PARC E80 Experiment, 2024,
http://ag.riken.jp/J-PARC/PAC/E80_TDR_2024_20240705_updated.pdf
- [3] K. Agari *et al.*, *Prog. Theor. Exp. Phys.*, Vol. 2012, p. 02B011, 2012
- [4] ATLAS TGC Collaboration, Amplifier-Shaper-Discriminator ICs and ASD Boards, Technical Report, ATLAS Internal Note MUON - NO - 1, 1999.